Published in final edited form as:
Eur J Neurosci. 2010 February ; 31(3): 463–476. doi:10.1111/j.1460-9568.2009.07058.x.

Nicotine facilitates LTP induction in oriens-lacunosum moleculare cells via Ca^{2+} entry through non-α7 nicotinic acetylcholine receptors

Yousheng Jia[1,*], **Yoshihiko Yamazaki**[1,2,*], **Sakura Nakauchi**[1], **Ken-Ichi Ito**[1,2], and **Katumi Sumikawa**[1]

[1] Department of Neurobiology and Behavior, University of California, Irvine, CA 92697-4550, USA

[2] Department of Neurophysiology, Yamagata University School of Medicine, Yamagata 990-9585, Japan

Abstract

Hippocampal inhibitory interneurons have a central role in the control of network activity, and excitatory synapses that they receive express Hebbian and anti-Hebbian long-term potentiation (LTP). Because many interneurons in the hippocampus express nicotinic acetylcholine receptors (nAChRs), we explored whether exposure to nicotine promotes LTP induction in these interneurons. We focused on a subset of interneurons in the stratum oriens/alveus that were continuously activated in the presence of nicotine due to the expression of non-desensitizing non-α7 nAChRs. We found that, in addition to α2 subunit mRNAs, these interneurons were consistently positive for somatostatin and neuropeptide Y mRNAs, and showed morphological characteristics of oriens-lacunosum moleculare cells. Activation of non-α7 nAChRs elevated intracellular Ca^{2+} levels at least in part via Ca^{2+} entry through their channels. Presynaptic tetanic stimulation induced *N*-methyl-D-aspartate receptor-independent LTP in voltage-clamped interneurons at −70 mV when in the presence, but not absence, of nicotine. Intracellular application of a Ca^{2+} chelator blocked LTP induction, suggesting the requirement of Ca^{2+} signal for LTP induction. The induction of LTP was still observed in the presence of ryanodine, which inhibits Ca^{2+}-induced Ca^{2+} release from ryanodine-sensitive intracellular stores, and the L-type Ca^{2+} channel blocker nifedipine. These results suggest that Ca^{2+} entry through non-α7 nAChR channels is critical for LTP induction. Thus, nicotine affects hippocampal network activity by promoting LTP induction in oriens-lacunosum moleculare cells via continuous activation of non-α7 nAChRs.

Keywords

rat; GABAergic interneurons; Ca^{2+} imaging; hippocampus; circuit plasticity

Introduction

Systemic administration of nicotine improves several hippocampal-dependent learning and memory tasks (Abdulla *et al*., 1996; Levin & Simon, 1998; Levin, 2002; Marti Barros *et al*., 2004; Gould, 2006; Dani & Bertrand, 2007; Davis *et al*., 2007; Kenney & Gould, 2008). However, little is known about the detailed mechanisms by which nicotine exerts its effects

Correspondence: Katumi Sumikawa, Department of Neurobiology and Behavior, University of California Irvine, CA 92697-4550, USA, Tel: (949) 824-5310, Fax: (949) 824-2447, ksumikaw@uci.edu.
*These authors contributed equally to this work.

on learning and memory. Long-term potentiation (LTP) of excitatory synaptic transmission is thought to be a cellular substrate of learning and memory. Thus, to gain insights into the mechanisms of nicotine's effects on learning and memory, some studies have been directed towards understanding its effects on LTP. Nicotine facilitates the induction of LTP at excitatory synapses on dentate granule cells (the perforant pathway) and CA1 pyramidal cells (the Schaffer collateral pathway) in the trisynaptic circuit of hippocampus (Sawada *et al*., 1994; Hamid *et al*., 1997; Fujii *et al*., 1999; Matsuyama *et al*., 2000; Ji *et al*., 2001; Mann & Greenfield, 2003; Welsby *et al*., 2006; Nakauchi *et al*., 2007a). In contrast, nicotine suppresses LTP induction at the temporoammonic pathway, a direct excitatory input from the entorhinal cortex to CA1 pyramidal cells, suggesting that nicotine influences LTP induction in a pathway-specific manner (Nakauchi *et al*., 2007a). It remains to be elucidated whether nicotine modulates LTP induction at excitatory synapses on interneurons in the hippocampus.

Nicotine's behavioral and cellular effects are mediated by its interaction with nicotinic acetylcholine receptors (nAChRs). In the hippocampus, at least 4 different nAChR subtypes, non-α7 (α2*, α3β4*, α4β2*) and α7 nAChRs, appear to be expressed (Alkondon *et al*., 2000; Alkondon & Albuquerque, 2001; McQuiston & Madison, 1999; Sudweeks & Yakel, 2000; Ji *et al*., 2001; Buhler & Dunwiddie, 2001, 2002; Frazier *et al*., 1998a, 1998b, 2003; Jia *et al*., 2009). The α7 nAChR, which is the most abundant subtype in the hippocampus, is highly Ca^{2+}-permeable (Seguela *et al*., 1993; Role & Berg, 1996) and, thus, has been proposed to contribute to synaptic plasticity. Indeed, activation of presynaptic or postsynaptic α7 nAChRs promotes LTP induction at the Schaffer collateral pathway via increasing glutamate release or stimulating Ca^{2+} signaling cascades, respectively (Ji *et al*., 2001). However, this subtype desensitizes in the presence of nicotine (Frazier *et al*., 1998a, 1998b; McQuiston & Madison, 1999; Alkondon *et al*., 2000; Alkondon & Albuquerque, 2005; Yamazaki *et al*., 2005, 2006). At the Schaffer collateral pathway, desensitization of postsynaptic α7 nAChRs on feedforward γ-aminobutyric acid (GABA)ergic interneurons can reduce feedforward inhibition via suppressing incoming excitatory nicotinic synaptic responses (Frazier *et al*., 1998a, 1998b; Yamazaki *et al*., 2005, 2006) and preventing Ca^{2+} signaling for inhibition of $GABA_A$ receptor-mediated responses (Wanaverbecq et al., 2007; Zhang & Berg, 2007). Suppression of feedforward inhibition could enhance *N*-methyl-D-aspartate receptor (NMDAR)-mediated responses in pyramidal cells (Bliss & Collingridge, 1993), providing a potential mechanism for the nicotine-induced facilitation of LTP induction via desensitization rather than activation of α7 nAChRs. It largely remains to be determined whether all of these mechanisms are working in concert during nicotine exposure to facilitate LTP induction. Activation of non-α7 nAChRs also suppresses feedforward inhibition via reducing GABA release and postsynaptic $GABA_A$ receptor-mediated responses (Yamazaki *et al*., 2005). The α4β2* nAChR subtype has the highest affinity for nicotine and is the primary candidate for mediating nicotine's effects. However, it is unknown whether this subtype is involved in nicotine-induced facilitation of LTP induction. The opposing effects of nicotine on LTP induction at Schaffer collateral and temporoammonic synapses are absent or greatly reduced in α2 knockout mice, suggesting that activation of this subtype differentially modulates LTP induction at these synapses (Nakauchi *et al*., 2007a). The α2* nAChR is the most sparsely expressed nAChR subtype in the brain, but shows a distinct localization in a subset of GABAergic interneurons in the stratum oriens/alveus (Wada *et al*., 1989; Ishii *et al*., 2005). A subset of oriens/alveus interneurons are continuously activated in the presence of nicotine, triggering interneuronal action potentials, which in turn causes the sustained release of GABA onto specific postsynaptic membrane domains (Jia *et al*., 2009). Thus, the nAChR subtype expressed in these interneurons becomes a critical component in hippocampal circuitry in the presence of nicotine, and potentially serves as a molecular switch for gating LTP via altering the local balance between excitation and inhibition.

GABAergic interneurons are distributed throughout all layers of the hippocampus and selectively innervate different domains of principal cells and other interneurons, providing a powerful control of circuit activity (Freund & Buzsaki, 1996). Thus, LTP at excitatory synapses on interneurons strongly influences the operation of hippocampal circuits. In addition to the modulation of circuit activity, activation of nAChRs on oriens/alveus interneurons may cause an increase in intracellular Ca^{2+} concentrations, which could in turn stimulate intracellular signaling for LTP induction. In the present study, we further characterized nicotine-sensitive oriens/alveus interneurons and explored the role of nAChRs in LTP induction in these interneurons.

Materials and Methods

All animal procedures were conducted in accordance with the National Institutes of Health *Guide for the Care and Use of Laboratory Animals* and with protocols approved by the Institutional Animal Care and Use Committee of the University of California at Irvine. Efforts were made to minimize numbers of animals used.

Slice preparation

Sprague-Dawley rats (18- to 54-day-old; Harlan, Indianapolis, IN, USA) were anesthetized with urethane (1.25 g/kg) and killed by decapitation. Transverse hippocampal slices (375 μm) were prepared and maintained at 30–32°C in artificial cerebrospinal fluid containing (in mM): NaCl 124, KCl 5, NaH_2PO_4 1.25, $MgSO_4$ 2, $CaCl_2$ 2.5, $NaHCO_3$ 22, and glucose 10 and oxygenated with 95% O_2/5% CO_2, for at least 1 hour before recordings.

Electrophysiological recordings

Current- and voltage-clamp recordings were made from the somatic region of pyramidal cells and interneurons as described previously (Yamazaki *et al*., 2005, 2006). Slices were placed in a recording chamber, submerged, and continuously perfused at 2–3 ml/min with oxygenated artificial cerebrospinal fluid at 30°C. Neurons were visualized using a 40x water-immersion objective, infrared differential interference contrast (IR-DIC) system (Axioskop, Zeiss, Germany), and a charge-coupled device camera C2400 (Hamamatsu Corporation, Hamamatsu, Japan). Patch electrodes were pulled from borosilicate glass (World Precision Instruments, Sarasota, FL, USA) using a micropipette puller (P-97, Sutter Instrument, Novato, CA, USA). The pipettes had a resistance of 3–8 MΩ after being filled with pipette solution. For voltage-clamp recordings, pipette solution contained (in mM) 117 Cs-methanesulfonate, 10 HEPES, 0.5 EGTA, 2.8 NaCl, 5 TEA-Cl, 5 QX-314, 2.5 Mg-ATP, and 0.3 Na-GTP, adjusted to pH 7.3 with CsOH. For current clamp recordings, pipette solution contained (in mM) 140 K-gluconate, 10 HEPES, 0.5 EGTA, 10 NaCl, 1 $MgCl_2$, 2 Mg-ATP, 0.2 Na-GTP, and QX-314, adjusted to pH 7.3 with KOH. The series resistance, normally about 15–20 MΩ, was monitored throughout the experiment; if it changed more than 20%, the recording was discarded. Responses of currents and potentials were recorded using Axopatch-200B or Axoclamp-2B (Axon Instruments, Union City, CA, USA), and were filtered (1–2 kHz), digitized at 1–5 kHz, and stored on a computer. In LTP experiments, excitatory postsynaptic currents (EPSCs) were evoked in oriens/alveus interneurons using a fine tip bipolar tungsten stimulating electrode (TT201-029, Unique Medical, Tokyo, Japan), which was positioned approximately 100–150 μm from the recorded cell. Because there was a possibility that EPSCs contained not only monosynaptic EPSCs but also polysynaptic responses, we measured the amplitude of the first negative peak to evaluate changes in monosynaptic EPSCs. When the amplitude of monosynaptic EPSCs could not be measured accurately due to overlap with a second EPSC peak or an unusual long EPSC peak latency, the recording was discarded. We also applied the NMDAR

antagonist 2-amino-5-phosphopentanoate (AP5; 50 μM) throughout recordings to prevent a possible passively propagated form of LTP in interneurons.

Calcium imaging

For simultaneous Ca^{2+} imaging and electrophysiological recordings, interneurons were first loaded with the calcium indicator calcium green 1 (100 μM; Molecular Probes, Eugene, OR, U.S.A.) via the recording pipette. It was allowed to diffuse for a minimum of 20 min before starting optical and electrophysiological recordings. Fluorescence images were obtained by using MetaMorph Imaging System (Universal Imaging Corporation, West Chester PA, USA) and a fluorescent microscope (Axioskop, Zeiss) equipped with a mercury lamp, 488-nm excitation and 520-nm emission filters, and a charge-coupled device camera M4314 (Hamamatsu Corporation). Fluorescence intensities (F_{post}) over the region of interest in the soma at a given time point were normalized to baseline values [expressed as $\%\Delta F/F = (F_{post} - F_{rest})/(F_{rest} - F_{back}) \times 100$, where F_{rest} is the baseline fluorescence and F_{back} is the background fluorescence measured outside the cell] and plotted against time. To monitor the responsiveness of interneurons at the beginning and end of experiments, they were depolarized by 15mV by a current injection to generate calcium responses via activation of voltage-dependent Ca^{2+} channels.

Biocytin staining

During whole-cell recording, interneurons were passively filled with biocytin (0.5%) through the recording pipette for subsequent morphological identification (dendrite orientation, somata shape, and axon distribution) of interneurons. Following recordings, slices were incubated for 30 min and fixed overnight in 0.1 M phosphate buffer (PB, pH 7.4) containing 4% paraformaldehyde and 0.05% glutaraldehyde. Biocytin staining was processed using an avidin-peroxidase reaction (Vectastain ABC Standard Kit, Vector, Burlingame,CA, USA) with 3,3′-diaminobenzidine. The slice was then mounted on gelatin-coated glass slides for light microscopic examination.

Double-fluorescence immunohistochemistry

Hippocampal slices containing a biocytin-loaded interneuron were fixed by immersionin 4% paraformaldehyde in 0.1 M PB, pH 7.4, for several hours. After washing in 0.1 M PB, they were incubated with Alexa 546-conjugated streptavidin (Molecular Probes) diluted 1:500 with 0.1 M PB containing 0.1% Triton X-100 overnight at room temperature. Following washing in 0.1 M PB, the slices were incubated with an antibody against somatostatin-28 (IHC8004; Peninsula Laboratories, San Carlos, CA, USA; diluted 1:200) in 0.1 M PB containing 0.1% Triton X-100 for 10–12 h at room temperature. After washing, the slices were allowed to react with Alexa 488-conjugated goat anti-rabbit IgGs (Molecular Probes; diluted 1:500) in 0.1 M PB for 2 h at room temperature. The slices were then washed and coverslippedin Vectashield (Vector). Slices were observed under a confocal fluorescence microscope (LSM510 META, Zeiss).

In situ hybridization

The localization of α2 mRNA-positive cells by non-radioactive in situ hybridization was carried out as previously described (Ishii *et al*., 2005).

Single-cell reverse transcription (RT)-multiplex polymerase chain reaction (PCR)

To monitor the expression of molecular markers (calbindin D28k, parvalbumin, calretinin, neuropeptide Y, vasoactive intestinal polypeptide, somatostatin, and cholecystokinin) in recorded cells, single-cell RT-multiplex PCR was performed by a previously described procedure (Cauli *et al*., 1997). After recordings were completed, the cytoplasm of individual

neurons was harvested by applying suction on a patch pipette filled with sterile intracellular pipette solution. The contents of the pipette were expelled into a PCR tube by the application of positive pressure, quickly frozen on dry ice, stored at −80°C overnight, and subjected to RT-multiplex PCR using the Titan One Tube RT-PCR System (Roche Molecular Biochemicals, Indianapolis, IN, USA) and different pairs of PCR primers for simultaneous amplification of different molecular markers. This was followed by a second round of PCR using 1 μl of the first PCR product as a template. In this second round, each target cDNA was amplified individually using its specific primer pair. Each individual PCR reaction was run on an agarose gel and visualized with ethidium bromide for identification of target cDNAs.

Statistical analysis

Data were analyzed off-line using Mini analysis program (Synaptosoft Inc., Decatur, GA, USA), Origin (OriginLab, Northampton, MA, USA), and pCLAMP 7 (Axon Instruments). Data were expressed as means ± SEM. Sample size *n* refers to the number of neurons analyzed in electrophysiological or optical recordings from hippocampal slices. Significant changes in action potential firing frequency, membrane depolarization, Ca^{2+} response, EPSC amplitude (before vs. after drug application, or between two drug groups) were assessed using a paired or an unpaired, two-tailed Student's *t*-test where appropriate. The statistical tests for the data of Ca^{2+} response and LTP induction were carried out on the percentage data. These normalized data were compared using an unpaired *t*-test. The statistical tests for the data presented in Fig. 3D2 were carried out using one-way ANOVA and *a post hoc* Fisher test. A comparison was considered statistically significant if $P < 0.05$.

Results

Distribution of nicotine-sensitive interneurons in the stratum oriens/alveus We have previously found that a subset of interneurons in the stratum oriens/alveus were continuously excited in the presence of 0.2–1 μM nicotine (Jia *et al*., 2009), a concentration that can be achieved in the plasma during cigarette smoking (Benowitz et al., 1989; Henningfield *et al*., 1993), and were consistently positive for the α2 subunit mRNA by single-cell RT-PCR (Jia *et al*., 2009). To further characterize these interneurons, we carried out several experiments. Non-radioactive in situ hybridization histochemistry showed that α2 mRNA-positive cells were sparsely localized at the stratum oriens/alveus border (Fig. 1A), as reported previously (Ishii *et al*., 2005). Many of these cells appeared to possess a horizontally oriented soma, whereas a few cells displayed a vertically oriented soma (Fig. 1A). Based on this observation, under IR-DIC visualization, we targeted horizontally oriented interneurons at the stratum oriens/alveus border for whole-cell recording. We found that bath application of nicotine (0.2–10 μM) in the presence of the glutamate receptor antagonists 6, 7-dinitro-quinoxaline-2, 3-dione (DNQX; 20 μM) and AP5 (40 μM), which eliminate excitatory synaptic activity, depolarized the cells and triggered repetitive action potential firing in these interneurons. As reported previously (Jia *et al*., 2009), the frequency of action potentials increased in the presence of nicotine. On average, the application of 10 μM nicotine caused a maximum increase in the frequency of action potentials (Fig. 1B1–B3; control 0.05 ± 0.03 Hz vs. nicotine 4.91 ± 0.67 Hz, $n = 19$, $t_{18} = -7.27$, $P < 0.001$). The effect was sustained during application of nicotine and was blocked by the non-α7 nAChR antagonist dihydro-β-erythroidine (DHβE; 2 μM) (Fig. 1B1,B3; nicotine 4.91 ± 0.67 Hz vs. nicotine + DHβE 0.16 ± 0.05 Hz, $n = 19$, $t_{18} = 7.27$, $P < 0.001$). As reported previously (Jia *et al*., 2009), this effect of nicotine was not affected in the presence of the α7 nAChR antagonist methyllycaconitine (MLA; 100 nM, data not shown). These observations suggest that the location of α2 mRNA-positive cells at least partially overlaps with the distribution of nicotine-sensitive interneurons in the stratum oriens/alveus.

Under IR-DIC visualization, we observed that the soma of nicotine-sensitive interneurons was often, but not always, covered by perineuronal glial cells (Fig. 1C1), which were easily removed using gentle positive pressure before whole-cell recording, or associated with perineuronal glial cells (Fig. 1C2). These morphological features allowed us to identify many nicotine-sensitive interneurons before recording and, thus, approximately 80% of recorded cells were nicotine-sensitive.

Nicotine-sensitive interneurons are oriens-lacunosum moleculare cells

There are different subtypes of horizontally oriented interneurons in the stratum oriens/alveus, including oriens-lacunosum moleculare cells, basket cells, and oriens-bistratified cells (Freund & Buzsaki, 1996; Maccaferri, *et al*., 2000; Maccaferri, 2005). Basket cells are parvalbumin and cholecystokinin positive (Freund & Buzsaki, 1996; Maccaferri, *et al*., 2000). Both oriens-lacunosum moleculare cells and oriens-bistratified cells are somatostatin immunoreactive (Maccaferri, *et al*., 2000), and oriens-lacunosum moleculare cells also contain neuropeptide Y (Freund & Buzsaki, 1996). To gain insight into a nicotine-sensitive interneuron subtype, we combined patch-clamp recording and single-cell RT-multiplex PCR to monitor the differential expression of three calcium binding proteins (calbindin D28k, parvalbumin, and calretinin) and four neuropeptides (neuropeptide Y, vasoactive intestinal polypeptide, somatostatin, and cholecystokinin) that define interneuron types with partial overlaps (Freund & Buzsaki, 1996; Parra *et al*., 1998). To detect the mRNAs of these neurochemical markers simultaneously in a single cell, two steps of multiplex PCR were performed (Cauli *et al*., 1997; Jia *et al*., 2009). Initially, the efficiency and specificity of this protocol was tested on total RNA isolated from rat hippocampi. As Fig. 2A1 (top) shows, the seven specific mRNAs were detected, each generating a PCR product of the size predicted by its mRNA sequence. Subsequently, the differential expression of the seven markers was examined at the single cell level. We found that nicotine-sensitive interneurons were consistently positive for somatostatin and neuropeptide Y mRNAs (in 5 of 5 interneurons), and one of these neurons was positive for both calretinin and vasoactive intestinal polypeptide mRNAs (Fig. 2A1, bottom, and Fig. 2A2).

In a further effort to identify a nicotine-sensitive interneuron subtype, we passively filled these interneurons with biocytin through recording pipettes for subsequent morphological identification. All biocytin-filled cells had horizontally oriented dendrites. When axonal arborizations were visible (n = 10), they showed morphological characteristics of oriens-lacunosum moleculare cells (Fig. 2B), which project to the most distal dendrites of pyramidal cells (Freund & Buzsaki, 1996;Maccaferri *et al*., 2000;Maccaferri, 2005). To confirm the presence of somatostatin protein in nicotine-sensitive interneurons, some nicotine-responding interneurons were passively filled with biocytin for subsequent double-fluorescence immunohistochemistry with a somatostatin antibody. We found that biocytin-labeled cells were somatostatin-positive (Fig. 2C1, C2). These results demonstrate that nicotine-sensitive interneurons are oriens-lacunosum moleculare cells. However, because we were unable to follow the complete axonal arborization of some biocytin-filled interneurons, we cannot exclude the possibility that nicotine-responding interneurons include other subtypes of horizontally oriented interneurons, which express both somatostatin and neuropeptide Y.

Nicotine increases intracellular Ca^{2+} concentrations in oriens/alveus interneurons

Different subtypes of nAChRs are known to be differentially permeable to Ca^{2+} (Role & Berg, 1996; Fucile, 2004). Thus, activation of non-α7 nAChRs in oriens/alveus interneurons could elevate intracellular Ca^{2+} levels directly by being permeable to Ca^{2+} themselves, and indirectly by generating sufficient depolarizing current to activate voltage-dependent Ca^{2+} channels. Because increases in intracellular Ca^{2+} play a critical role in LTP induction

(Topolnik *et al*., 2005, 2006), we next examined whether nicotine causes an increase in intracellular Ca^{2+} levels. To measure changes in intracellular Ca^{2+} levels in the soma, we used a fluorescent assay with calcium green-1. Current-clamped cells were loaded with calcium green-1 via the patch pipette (Fig. 3A1, A2).

Subsequent bath application of nicotine (10 μM) in the presence of DNQX (20 μM) and AP5 (40 μM) produced detectable increases in fluorescent intensity at the soma, as shown in pseudocolor images (Fig. 3A2, A3). To determine whether the increased fluorescent intensity was due to the activation of non-α7 nAChRs, we simultaneously recorded nicotine-induced changes in membrane potential and fluorescent intensity in current-clamped cells. Bath application of nicotine (10 μM) induced a depolarization in interneurons (10.4 ± 1.2 mV, $n = 11$) and generated action potentials, which were completely blocked in the presence of DHβE (2 μM; Fig. 3B, C1; 0.2 ± 0.5 mV, $n = 9$, $t_{18} = -7.01$, $P < 0.001$). At the same time, bath application of nicotine (10 μM) increased Ca^{2+} responses (17.2 ± 3.1% increase over basal levels, $n = 11$), which were well maintained during nicotine-induced membrane depolarization, and this effect was almost completely inhibited in the presence of DHβE (2 μM; Fig. 3B, C2; 2.3 ± 0.6% increase over basal levels, $n = 9$, $t_{18} = -4.32$, $P < 0.001$). Reapplication of nicotine after approximately 10-min drug washout reproducibly induced interneuronal depolarization and intracellular Ca^{2+} rises (Fig. 3B, right). These results suggest that activation of non-α7 nAChRs causes increases in intracellular Ca^{2+} concentrations in these interneurons.

It has been shown that bath application of kainate caused depolarization and repetitive action potential firing in oriens-lacunosum moleculare cells (Cossart *et al*., 1998), which resembles the effects of nicotine on oriens/alveus interneurons (Jia *et al*., 2009). Thus, we next examined whether activation of kainate receptors induces Ca^{2+} rises in nicotine-sensitive oriens/alveus interneurons. Bath application of kainate (1 μM) induced a depolarization in interneurons (8.3 ± 1.7 mV, $n = 5$) and generated action potentials (Fig. 3D1,D2), and simultaneously increased Ca^{2+} responses (Fig. 3D1,D2; 14. 5 ± 4.4% increase over basal levels, $n = 5$). Changes in membrane potential and Ca^{2+} responses caused by application of kainite were very similar to those induced by application of nicotine (Fig. 3D2). Depolarizing the cells with 30 mM K^+ to activate voltage-dependent Ca^{2+} channels induced a membrane depolarization (Fig. 3D1,D2; 29.9 ± 3.2 mV, $n = 6$) that was significantly larger (Fig. 3D2; ANOVA, $F_{(2,19)} = 31.9$, $P < 0.001$) than that caused by nicotine ($P < 0.001$) or kainite ($P < 0.001$), and caused increases in Ca^{2+} responses (Fig. 3D1,D2; 28.3 ± 3.3% increase over basal levels, $n = 6$) that were significantly higher (Fig. 3D2; ANOVA, $F_{(2,19)} = 3.54$, $P = 0.049$) than the increases induced by nicotine ($P = 0.034$) or kainite ($P = 0.028$). Thus, nicotine-induced intracellular Ca^{2+} increases were much less than the Ca^{2+} increases that were produced by the activation of voltage-dependent Ca^{2+} channels. Ca^{2+} permeable α-amino-3-hydroxy-5-methylisoxazole-4-propionate receptors (AMPARs) are expressed in oriens/alveus interneurons (Topolnik et al., 2005, 2006; Kullmann, & Lamsa, 2007). In our experiments, these receptors, which could be activated by kainate, were not blocked. Thus, although kainate receptors can be Ca^{2+} permeable depending on the degree of post-transcriptional RNA editing of their subunits (Bernard *et al.* 1999; Lerma *et al.* 2001), the observed kainate-induced Ca^{2+} rises might be at least in part due to the activation of Ca^{2+} permeable AMPARs.

Non-α7 nAChRs on oriens/alveus interneurons are Ca^{2+} permeable

Our results described above demonstrate that activation of non-α7 nAChRs caused intracellular Ca^{2+} rises in oriens/alveus interneurons. However, it was unclear whether this was due to direct entry of Ca^{2+} through the receptor channel, depolarization-induced activation of voltage-dependent Ca^{2+} channels, or both. Initially, we attempted to pharmacologically dissect out the relative contribution of voltage-dependent Ca^{2+} channels

using Cd^{2+} as a voltage-gated Ca^{2+} channel blocker. We compared the amplitude of nicotine-induced Ca^{2+} elevations in current-clamped interneurons before and after addition of 100 μM Cd^{2+}, which almost completely blocked K^+ (30 mM) induced Ca^{2+} elevations (data not shown). However, we found that the inhibitory effect of Cd^{2+} on nicotine-induced Ca^{2+} rises was quite variable among different cells, perhaps due to differences in the relative contribution of voltage-dependent Ca^{2+} channels to a total Ca^{2+} elevation. Nevertheless, these experiments suggest the involvement of voltage-dependent Ca^{2+} channels in nicotine's effects. Subsequently, we decided to simply determine whether nicotine increases intracellular Ca^{2+} concentrations without the contribution of voltage-dependent Ca^{2+} channels. Thus, we measured nicotine-induced Ca^{2+} responses in interneurons, which were voltage-clamped below the threshold for activation of voltage-dependent Ca^{2+} channels. Interneurons were loaded with calcium green-1 via the patch pipette and the cells were voltage-clamped at −70 mV in the presence of DNQX (20 μM), AP5 (40 μM). Simultaneous measurements of currents and Ca^{2+} responses were carried out. As reported previously (Jia *et al*., 2009), bath application of nicotine (0.5–10 μM) produced long-lasting inward currents that were inhibited by DHβE, but not MLA (data not shown). On average, the application of 10 μM nicotine caused a maximum response (Fig. 4A, top, 87.9 ± 2.0 pA, $n = 6$). Bath application of nicotine (10 μM) also produced a fluorescence response (Fig. 4A, bottom, B; 9.9 ± 1.3% increase over basal levels, $n = 6$), suggesting that activation of non-α7 nAChRs can produce increases in intracellular Ca^{2+} levels by direct passage of Ca^{2+} through the receptor channel. The response kinetics were different between current-clamped and voltage-clamped conditions (Fig. 3B and Fig. 4A). Furthermore, the increase of intracellular Ca^{2+} concentrations in voltage-clamped cells was smaller than that observed in current-clamped cells, although the difference did not reach statistical significance (Fig. 4B; $t_{15} = 1.69$, $P = 0.11$). These observations further support the idea that depolarization-induced activation of voltage-dependent Ca^{2+} channels via non-α7 nAChRs contributes to nicotine-induced intracellular Ca^{2+} rises in current-clamped cells.

Nicotine facilitates LTP induction at excitatory synapses on oriens/alveus interneurons

Many interneurons in the stratum oriens/alveus, including oriens-lacunosum moleculare cells, show NMDAR-independent LTP (Perez *et al.*, 2001; Lapointe *et al.*, 2004; Topolnik *et al*., 2006; Lamsa *et al.*, 2007; Kullmann & Lamsa, 2008; Oren *et al*., 2009), which can be induced by different LTP induction protocols. To examine whether nicotine facilitates the induction of LTP in oriens/alveus interneurons, we recorded EPSCs in voltage-clamped cells (at −70 mV). Most of the excitatory input to oriens-lacunosum moleculare cells arises from recurrent collaterals of CA1 pyramidal cells. Thus, we evoked EPSCs by stimulation in the stratum oriens, close to the patched interneurons (Fig. 5A). Tetanic stimulation (100 Hz, 100 pulses) was used to induce LTP under voltage-clamp conditions. Although NMDA receptor-dependent LTP does not occur in oriens/alveus interneurons (Perez *et al.* 2001; Lamsa *et al.* 2007), NMDAR-dependent LTP occurring at the Schaffer collateral-pyramidal cell synapses can passively propagate to these interneurons (Perez *et al.* 2001). Thus, to prevent a possible passively propagated form of LTP in interneurons, all recordings were performed in the presence of the NMDAR antagonist AP5 (50 μM). In addition, bicuculline (10 μM), MLA (50 nM), and atropine (1μM) were added to the bath perfusate to block $GABA_A$ receptors, α7 nAChRs, and muscarinic receptors, respectively. Under these conditions, tetanic stimulation failed to induce LTP (Fig. 5B,F; 104.3 ± 8.3% 50–55 min after tetanus, $n = 4$) in voltage-clamped interneurons. However, when tetanic stimulation was applied in the presence of nicotine (10 μM), LTP was induced (Fig. 5C,F; 153.3 ± 14.8% 50–55 min after tetanus, $n = 4$; tetanus alone vs. tetanus + 10 μM nicotine, $t_6 = 3.15$, $P = 0.020$). We have previously reported that bath application of nicotine (0.5–1 μM) produced long-lasting inward currents (10–47 pA) in oriens/alveus interneurons (Jia *et al*., 2009). Thus, we next examined whether a lower concentration (1 μM) of nicotine facilitates LTP induction in

oriens/alveus interneurons, and found that LTP was induced in nicotine-responding interneurons (Fig. 5D,F; 139.4 ± 14.8% 50–55 min after tetanus, $n = 5$; tetanus alone vs. tetanus + 1 μM nicotine, $t_7 = 2.63$, $P = 0.033$). Bath application of nicotine for 1.5 min caused decreases in the amplitude of EPSCs and increases in holding current, indicating the presence of nicotine-induced inward currents (Fig. 5C,D). Increases in holding current reached its peak value in approximately 3 min after nicotine application, at which time the tetanus was delivered, and returned to a baseline level following washout of nicotine. The time course of changes in EPSC amplitude following nicotine application mirrored that of changes in holding current that occurred after nicotine application. This suggests that nicotine-induced inward currents suppresses EPSCs, perhaps due to reduced driving force for Na^+ and decreased membrane resistance, which causes a shunting effect. To exclude the possibility that the observed effect of nicotine on LTP induction was due to a long-lasting effect of nicotine, we next examined the effect of nicotine alone (i.e., without tetanic stimulation) on EPSCs. Bath application of nicotine (10 μM) for 1.5 min caused decreases in the amplitude of EPSCs, reaching its minimum in approximately 3 min after nicotine application and returning to basal levels following washout of nicotine (Fig. 5E,F; 105.5 ± 6.1% 53–58 min after nicotine application, $n = 4$; tetanus + nicotine vs. nicotine alone, $t_6 = 3.45$, $P = 0.017$). Thus, nicotine alone had no long-lasting effect on EPSCs. These results suggest that nicotine facilitates the induction of LTP in oriens/alveus interneurons via activation of non-α7 nAChRs.

Ca^{2+} entry through non-α7 nAChR channels facilitates LTP induction in oriens/alveus interneurons

Because increases in intracellular Ca^{2+} concentrations have a critical role in LTP induction in oriens/alveus interneurons (Topolnik *et al*., 2006), we next examined whether Ca^{2+} entry through non-α7 nAChR channels was responsible for the nicotine-induced facilitation of LTP induction. To exclude the contribution of voltage-dependent Ca^{2+} channels, we recorded EPSCs in voltage-clamped oriens/alveus interneurons (at −70 mV) in the presence of AP5 (50 μM), bicuculline (10 μM), MLA (50 nM), and atropine (1μM). Tetanic stimulation was used to induce LTP under voltage-clamp conditions. We first examined the role of Ca^{2+} while recording from voltage-clamped interneurons with a pipette containing a high concentration of the Ca^{2+} chelator BAPTA (10 mM). Intracellular application of BAPTA blocked the nicotine-induced facilitation of LTP induction (Fig. 6A,E; 102.3 ± 13.0% 50–55 min after tetanus, $n = 4$; nicotine vs. nicotine + BAPTA, $t_6 = 2.80$, $P = 0.031$). Under these conditions, nicotine still elicited inward current as evidenced by the increase in holding currents (Fig. 6A, bottom). This suggests that the nicotine-induced facilitation of LTP induction requires Ca^{2+} entry through non-α7 nAChRs in patched interneurons. To explore the contribution of other Ca^{2+} sources to the nicotine-induced facilitation of LTP induction, we carried out pharmacological experiments. Nicotine-induced enhancement of LTP in the rat dentate gyrus is dependent on entry of Ca^{2+} via L-type Ca^{2+} channels and Ca^{2+} release from ryanodine-sensitive intracellular stores (Welsby *et al*., 2006). Therefore, nicotine-induced enhancement of LTP is prevented by the blockers nifedipine and ryanodine, respectively. Because the interneurons were voltage-clamped at −70 mV, it was very unlikely that nicotine-induced responses activated voltage-dependent Ca^{2+} channels. However, to completely exclude the involvement of L-type Ca^{2+} channels, we examined the effect of nifedipine (30 μM) on nicotine-induced facilitation of LTP induction. As expected, we found that nifedipine (30 μM) did not have a significant effect on the nicotine-induced facilitation of LTP induction (Fig. 6B,E; 146.6 ± 10.6% 50–55 min after tetanus, $n = 4$; nicotine vs. nicotine + nifedipine, $t_6 = 0.01$, $P = 0.99$), demonstrating that Ca^{2+} entry via L-type voltage-dependent Ca^{2+} channels is not involved in the effect. Another possible source of Ca^{2+} contributing to LTP induction is Ca^{2+}-induced Ca^{2+} release (CICR). Ca^{2+} entry through nAChR channels can be coupled to CICR (Dajas-Bailador and Wonnacott, 2004),

and CICR has been linked to LTP in oriens/alveus interneurons (Topolnik *et al*., 2006). Thus, we examined the possible contribution of ryanodine-sensitive internal Ca^{2+} stores to nicotine's effects, and found that blockade of CICR with ryanodine had no significant effect on nicotine-induced facilitation of LTP induction (Fig. 6C–E; 10 μM ryanodine, 166.7 ± 14.1% 50–55 min after tetanus, $n = 4$; nicotine vs. nicotine + 10 μM ryanodine, $t_6 = 0.41$, $P = 0.69$; 100 μM ryanodine, 171.2 ± 17.8% 50–55 min after tetanus, $n = 4$; nicotine vs. nicotine + 100 μM 2+ ryanodine, $t_6 = 0.88$, $P = 0.41$). These results suggest that the major source of Ca contributing to the nicotine-induced facilitation of LTP induction is via non-α7 nAChR channels.

Discussion

The present study demonstrates that horizontally oriented interneurons at the stratum oriens/alveus border contain Ca^{2+}-permeable non-α7 nAChRs, which are continuously activated in the presence of nicotine, and their activation facilitates the induction of LTP in these interneurons. Most, if not all, of these interneurons appeared to be oriens-lacunosum moleculare cells, which provide feedback inhibition onto the distal dendrites of pyramidal cells. Oriens-lacunosum moleculare cells are thought to be involved in the generation of theta oscillations, which typically occurs during exploratory activity, and are silenced during sharp wave ripples, which have been implicated in memory consolidation (Gillies *et al*., 2002; Klausberger et al., 2003; Somogyi & Klausberger, 2005; Kullmann & Lamsa, 2007). Thus, sustained activation of oriens-lacunosum moleculare cells in the presence of nicotine and LTP induction in these cells via non-α7 nAChRs may affect naturally occurring network activity, and thereby learning and memory.

A non-α7 nAChR subtype expressed in nicotine-sensitive oriens/alveus interneurons

It was previously reported that horizontally oriented interneurons in the stratum oriens/alveus, including oriens-lacunosum moleculare cells, contained both α7 and non-α7 nAChRs, which were activated by ACh puffs but were desensitized in the presence of nicotine (Frazier *et al*., 1998a; McQuiston & Madison, 1999; Sudweeks & Yakel, 2000). Because it was not tested whether bath application of nicotine elicited non-α7 nAChR-mediated responses in these interneurons, whether these interneurons expressed slowly or non-desensitizing nAChR subtype was unclear. Furthermore, single-cell RT-PCR analysis showed that these interneurons were consistently positive for all α subunit subtypes (α2-α7 mRNAs), making it difficult to identify a non-α7 nAChR subtype that mediated the responses (Sudweeks & Yakel, 2000). Our previous study demonstrated that bath application of nicotine produced slow inward currents in a subset of horizontally oriented interneurons in the stratum oriens/alveus, which were well maintained and inhibited by the non-α7 antagonist DHβE, but not the α7 antagonist MLA (Jia *et al*., 2009). In situ hybridization demonstrate that the α2 mRNA is uniquely expressed in a subset of interneurons in the stratum oriens/alveus (Ishii *et al*., 2005; Jia *et al*., 2009). Furthermore, single-cell RT-PCR analysis demonstrated that these nicotine-responding interneurons were consistently positive for the α2 subunit mRNA (in 8 of 8 interneurons) and two of these cells were positive for the α3 subunit mRNA, but not other α subunit mRNAs (Jia *et al*., 2009). Thus, the nicotine-induced facilitation of LTP induction is most likely mediated via activation of α2* nAChRs. However, the absence of α3 and α4 subunit mRNAs in many or all nicotine-sensitive interneurons, respectively, can easily be due to a lack of the sensitivity needed to detect less-abundant nAChR subunit mRNAs than α2 subunit mRNAs in these interneurons. It remains to be determined whether these cells contain functional α2* nAChRs that mediate the effects of nicotine.

An interneuron subtype containing non-desensitizing non-α7 nAChRs

The present study demonstrated that biocytin-filled nicotine-sensitive cells showed morphological characteristics of oriens-lacunosum moleculare cells, when axonal arborizations were visible. Furthermore, all non-α7 nAChR-containing interneurons tested in the present study were positive for somatostatin and neuropeptide Y, both of which are known to be expressed in oriens-lacunosum moleculare cells (Freund & Buzsaki, 1996; Maccaferri *et al*., 2000).

Nicotine-sensitive horizontally oriented interneurons in the stratum oriens/alveus are connected to pyramidal cells (Jia *et al*., 2009). In the literature (Freund & Buzsaki, 1996; Maccaferri *et al*., 2000; Maccaferri, 2005), at least three different subtypes of horizontally oriented interneurons (oriens-lacunosum moleculare cells, basket cells, and oriens-bistratified cells) that innervate pyramidal cells have been identified and characterized. Both oriens-lacunosum moleculare cells and oriens-bistratified cells are somatostatin immunoreactive, but basket cells, which innervate the soma, are not (Freund & Buzsaki, 1996; Maccaferri *et al*., 2000). Thus, although rigid classification of the subtypes of interneurons may be difficult, it is most likely that interneurons activated by nicotine are not basket cells. Because a previous study demonstrated that non-α7 nAChR-mediated responses in oriens-lacunosum moleculare cells desensitized in the presence of nicotine (McQuiston & Madison, 1999), our results suggest the presence of a separate population of oriens-lacunosum moleculare cells, expressing non-desensitizing non-α7 nAChRs.

Oriens-lacunosum moleculare cells project to the most distal dendrites of pyramidal cells where the temporoammonic path terminates (Freund & Buzsaki, 1996; Maccaferri *et al*., 2000; Maccaferri, 2005). Bath application of nicotine inhibits field excitatory postsynaptic potentials at the temporoammonic pathway, which requires GABAergic inhibition (Nakauchi *et al*., 2007a,b). This effect of nicotine is prevented, if a knife cut is made along the pyramidal layer in the stratum oriens to sever the axons of interneurons projecting to the apical dendrites of pyramidal cells (Nakauchi *et al*., 2007b). These observations suggest that the effect of nicotine is attributed to GABA release from the terminals of oriens-lacunosum moleculare cells. The axons of oriens-bistratified cells primarily terminate in the stratum radiatum and overlap the dendritic trees of pyramidal cells (Maccaferri *et al*., 2000). Bath application of nicotine has no significant effect on field excitatory postsynaptic potentials at the Schaffer collateral pathway (Fujii *et al*., 1999; Nakauchi *et al*., 2007a), suggesting that there is no significant GABA release from the terminals of oriens-bistratified cells during nicotine application. These observations also support the idea that oriens-lacunosum moleculare cells are a major subtype of nicotine-sensitive interneurons in the stratum oriens/alveus, which express α2 mRNAs. Identification of a nicotine-sensitive interneuron subtype as an oriens-lacunosum moleculare cell is significant, because nicotine-induced tonic inhibition at the most distal dendrites would depress direct information flow into CA1 pyramidal cells from entorhinal input (the temporoammonic path) and might preferentially direct information flow to CA1 pyramidal cells through the trisynaptic circuitry in the presence of nicotine.

Roles of Ca^{2+} entering through nAChR channels in circuit activity and plasticity

The α7 nAChR is expressed at high levels by interneurons in the hippocampal CA1 region (Alkondon & Albuquerque, 2001; Alkondon *et al*., 2000; McQuiston & Madison, 1999; Sudweeks & Yakel, 2000; Ji *et al*., 2001; Buhler & Dunwiddie, 2001, 2002; Frazier *et al*., 1998a, 1998b, 2003), in which activation of α7 nAChRs causes an increase in intracellular Ca^{2+} concentrations without involving CICR or activation of voltage-dependent Ca^{2+} channels (Khiroug *et al*., 2003; Fayuk & Yakel., 2005, 2007). This source of Ca^{2+} triggers

signaling, leading to the suppression of $GABA_A$ receptor-mediated responses in the interneurons (Wanaverbecq et al., 2007; Zhang & Berg, 2007).

Oriens/alveus interneurons in the hippocampal CA1 region express non-α7 nAChRs, which desensitize in the presence of nicotine (McQuiston & Madison, 1999). The activation of these non-α7 nAChRs via 5 sec pressure pulses of ACh (2 mM) in the presence of MLA does not significantly change intracellular Ca^{2+} concentrations (Fayuk & Yakel., 2005). However, in the present study, we found that bath application of nicotine increases Ca^{2+} levels in nicotine-sensitive interneurons at the stratum oriens/alveus border. This increase is at least in part attributed to Ca^{2+} entry through non-α7 nAChRs, which are continuously activated in the presence of nicotine. The change in intracellular Ca^{2+} concentrations caused by a brief activation of non-α7 nAChRs in oriens/alveus interneurons may be too small to be detected, and only becomes detectable when they are continuously activated in the presence of nicotine. In this case, Ca^{2+} signals leading to LTP induction can be only elicited in interneurons expressing non-desensitizing non-α7 nAChRs, because they are continuously activated in the presence of nicotine.

Nicotine-induced facilitation of LTP induction in oriens/alveus interneurons

Oriens/alveus interneurons show both Hebbian and anti-Hebbian forms of LTP, both of which are independent of the activation of NMDARs and appear to be expressed presynaptically (Perez *et al.*, 2001; Lapointe *et al.*, 2004; Lamsa *et al.*, 2007; Kullmann & Lamsa, 2007). In the present study, high frequency presynaptic stimulation with the activation of non-α7 nAChRs induced LTP in oriens/alveus interneurons that were voltage-clamped at −70 mV. Thus, this LTP, which is also independent of the activation of NMDARs, is arguably anti-Hebbian.

Nicotine-induced LTP in oriens/alveus interneurons requires postsynaptic Ca^{2+} rises, as in the cases of Hebbian and anti-Hebbian forms of LTP, both of which occur at synapses containing Ca^{2+} permeable AMPARs (Perez et al., 2001; Lapointe et al., 2004; Lamsa *et al.*, 2007; Kullmann & Lamsa, 2007). The mGluR1a subtype is highly expressed in oriens/alveus interneurons (Masu *et al*., 1991; Lujan et al., 1996) and can be activated synaptically (Huang *et al*., 2004). Activation of this subtype induces Ca^{2+} influx via transient receptor potential channels and Ca^{2+} release from intracellular stores (Topolnik *et al*., 2006). These sources of Ca^{2+} contribute to a Hebbian form of LTP (Topolnik *et al*., 2006). A well-established pathway of mGluR1 Ca^{2+} signaling is 1,4,5-trisphosphate-dependent intracellular Ca^{2+} release (Pin & Duvoisin, 1995). However, because 1,4,5-trisphosphate receptors appear to be absent in oriens/alveus interneurons (Fotuhi *et al.*, 1993), mGluR1/5-mediated Ca^{2+} signaling in these interneurons involves Ca^{2+} release from ryanodine-sensitive Ca^{2+} stores (Woodhall *et al.*, 1999). This source of Ca^{2+} appears to be also necessary for anti-Hebbian forms of LTP induction (Lamsa *et al.*, 2007). In contrast, this source of Ca^{2+} appears to be unnecessary for nicotine-induced LTP induction, because it still occurs after ryanodine receptors are blocked. One possible explanation is that Ca^{2+} from ryanodine-sensitive Ca^{2+} stores lowers the threshold for LTP induction, but is not required for LTP induction when in the presence of Ca^{2+} entering through non-α7 nAChRs. The relative contribution of different Ca^{2+} signals, arising from Ca^{2+} permeable AMPARs and non-α7 nAChRs, to LTP induction remains to be determined.

Oriens-lacunosum moleculare cells receive excitatory synaptic input from the recurrent collaterals of CA1 pyramidal cells, which fire at high frequency during sharp wave ripple activity (Klausberger *et al*., 2003; Somogyi & Klausberger, 2005; Kullmann & Lamsa, 2007). As suggested by others, this network activity may trigger LTP induction in oriens-lacunosum moleculare cells (Kullmann & Lamsa, 2007). Because the nicotine levels achieved after smoking can continuously activate oriens-lacunosum moleculare cells,

smoking may affect hippocampal network activity by promoting a long-term alteration of pyramidal cell excitation of these cells.

Acknowledgments

This research was supported by the National Institute on Drug Abuse (DA014542, DA025269, DA026458).

Abbreviations

ACh	acetylcholine
AMPAR	α-amino-3-hydroxy-5-methylisoxazole-4-propionate receptor
AP5	2-amino-5-phosphopentanoate
CICR	Ca^{2+}-induced Ca^{2+} release
DHβE	dihydro-β-erythroidine
DNQX	6, 7-dinitroquinoxaline-2, 3-dione
EPSCs	excitatory postsynaptic currents
GABA	γ-aminobutyric acid
IR-DIC	infrared-differential interference contrast
LTP	long-term potentiation
mGluRs	metabotropic glutamate receptors
MLA	methyllycaconitine
nAChRs	nicotinic acetylcholine receptors
NMDARs	*N*-methyl-D-aspartate receptors
PB	phosphate buffer
PCR	polymerase chain reaction
RT	reverse transcription

References

Abdulla FA, Bradbury E, Calaminici MR, Lippiello PM, Wonnacott S, Gray JA, Sinden JD. Relationship between up-regulation of nicotine binding sites in rat brain and delayed cognitive enhancement observed after chronic or acute nicotinic receptor stimulation. Psychopharmacology. 1996; 124:323–331. [PubMed: 8739547]

Alkondon M, Pereira EF, Almeida LE, Randall WR, Albuquerque EX. Nicotine at concentrations found in cigarette smokers activates and desensitizes nicotinic acetylcholine receptors in CA1 interneurons of rat hippocampus. Neuropharmacology. 2000; 39:2726–2739. [PubMed: 11044743]

Alkondon M, Albuquerque EX. Nicotinic acetylcholine receptor alpha7 and alpha4beta2 subtypes differentially control GABAergic input to CA1 neurons in rat hippocampus. J Neurophysiol. 2001; 86:3043–55. [PubMed: 11731559]

Alkondon M, Albuquerque EX. Nicotinic receptor subtypes in rat hippocampal slices are differentially sensitive to desensitization and early in vivo functional up-regulation by nicotine and to block by bupropion. J Pharmacol Exp Ther. 2005; 313:740–750. [PubMed: 15647329]

Benowitz NL, Porchet H, Jacob P. Nicotine dependence and tolerance in man: pharmacokinetic and pharmacodynamic investigations. Prog Brain Res. 1989; 79:279–287. [PubMed: 2587748]

Bernard A, Ferhat L, Dessi F, Charton G, Represa A, Ben-Ari Y, Khrestchatisky M. Q/R editing of the rat GluR5 and GluR6 kainate receptors in vivo and in vitro: evidence for independent

developmental, pathological and cellular regulation. Eur J Neurosci. 1999; 11:604–616. [PubMed: 10051761]

Bliss TVP, Collingridge GL. A synaptic model of memory: long-term potentiation in the hippocampus. Nature. 1993; 361:31–39. [PubMed: 8421494]

Buhler AV, Dunwiddie TV. alpha7 nicotinic acetylcholine receptors on GABAergic interneurons evoke dendritic and somatic inhibition of hippocampal neurons. J Neurophysiol. 2002; 87:548–557. [PubMed: 11784770]

Cauli B, Audinat E, Lambolez B, Angulo MC, Ropert N, Tsuzuki K, Hestrin S, Rossier J. Molecular and physiological diversity of cortical nonpyramidal cells. J Neurosci. 1997; 17:3894–3906. [PubMed: 9133407]

Cossart R, Esclapez M, Hirsch JC, Bernard C, Ben-Ari Y. GluR5 kainate receptor activation in interneurons increases tonic inhibition of pyramidal cells. Nat Neurosci. 1998; 1:470–478. [PubMed: 10196544]

Dani JA, Bertrand D. Nicotinic acetylcholine receptors and nicotinic cholinergic mechanisms of the central nervous system. Annu Rev Pharmacol Toxicol. 2007; 47:699–729. [PubMed: 17009926]

Davis JA, Kenney JW, Gould TJ. Hippocampal alpha4beta2 nicotinic acetylcholine receptor involvement in the enhancing effect of acute nicotine on contextual fear conditioning. J Neurosci. 2007; 27:10870–10877. [PubMed: 17913920]

Fayuk D, Yakel JL. Ca^{2+} permeability of nicotinic acetylcholine receptors in rat hippocampal CA1 interneurones. J Physiol (Lond). 2005; 566:759–768. [PubMed: 15932886]

Fayuk D, Yakel JL. Dendritic Ca^{2+} signalling due to activation of alpha 7-containing nicotinic acetylcholine receptors in rat hippocampal neurons. J Physiol (Lond). 2007; 582:597–611. [PubMed: 17510177]

Fotuhi M, Sharp AH, Glatt CE, Hwang PM, von Krosigk M, Snyder SH, Dawson TM. Differential localization of phosphoinositide-linked metabotropic glutamate receptor (mGluR1) and the inositol 1,4,5-trisphosphate receptor in rat brain. J Neurosci. 1993; 13:2001–2012. [PubMed: 8386753]

Frazier CJ, Rollins YD, Breese CR, Leonard S, Freedman R, Dunwiddie TV. Acetylcholine activates an α-bungarotoxin-sensitive nicotinic current in rat hippocampal interneurons, but not pyramidal cells. J Neurosci. 1998a; 18:1187–1195. [PubMed: 9454829]

Frazier CJ, Buhler AV, Weiner JL, Dunwiddie TV. Synaptic potentials mediated via α-bungarotoxin-sensitive nicotinic acetylcholine receptors in rat hippocampal interneurons. J Neurosci. 1998b; 18:8228–8235. [PubMed: 9763468]

Frazier CJ, Strowbridge BW, Papke RL. Nicotinic receptors on local circuit neurons in dentate gyrus: a potential role in regulation of granule cell excitability. J Neurophysiol. 2003; 89:3018–3028. [PubMed: 12611982]

Freund TF, Buzsaki G. Interneurons of the hippocampus. Hippocampus. 1996; 6:347–470. [PubMed: 8915675]

Fucile S. Ca^{2+} permeability of nicotinic acetylcholine receptors. Cell Calcium. 2004; 35:1–8. [PubMed: 14670366]

Fujii S, Ji Z, Morita N, Sumikawa K. Acute and chronic nicotine exposure differentially facilitate the induction of LTP. Brain Res. 1999; 846:137–143. [PubMed: 10536221]

Gillies MJ, Traub RD, LeBeau FE, Davies CH, Gloveli T, Buhl EH, Whittington MA. A model of atropine-resistant theta oscillations in rat hippocampal area CA1. J Physiol (Lond). 2002; 543:779–793. [PubMed: 12231638]

Gould TJ. Nicotine and hippocampus-dependent learning: implications for addiction. Mol Neurobiol. 2006; 34:93–107. [PubMed: 17220532]

Hamid S, Dawe GS, Gray JA, Stephenson JD. Nicotine induces long-lasting potentiation in the dentate gyrus of nicotine-primed rats. Neurosci Res. 1997; 29:81–85. [PubMed: 9293495]

Henningfield JE, Stapleton JM, Benowitz NL, Grayson RF, London ED. Higher levels of nicotine in arterial than in venous blood after cigarette smoking. Drug Alcohol Depend. 1993; 33:23–29. [PubMed: 8370337]

Huang YH, Sinha SR, Tanaka K, Rothstein JD, Bergles DE. Astrocyte glutamate transporters regulate metabotropic glutamate receptor-mediated excitation of hippocampal interneurons. J Neurosci. 2004; 24:4551–4559. [PubMed: 15140926]

Ishii K, Wong JK, Sumikawa K. A comparison of α2 nicotinic acetylcholine receptor subunit mRNA expression in the central nervous system of rats and mice. J Comp Neurol. 2005; 493:241–260. [PubMed: 16255031]

Ji D, Lape R, Dani JA. Timing and location of nicotinic activity enhances or depresses hippocampal synaptic plasticity. Neuron. 2001; 31:131–141. [PubMed: 11498056]

Jia Y, Yamazaki Y, Nakauchi S, Sumikawa K. Alpha2 nicotine receptors function as a molecular switch to continuously excite a subset of interneurons in rat hippocampal circuits. Eur J Neurosci. 2009; 29:1588–1603. [PubMed: 19385992]

Kenney JW, Gould TJ. Modulation of hippocampus-dependent learning and synaptic plasticity by nicotine. Mol Neurobiol. 2008; 38:101–121. [PubMed: 18690555]

Khiroug L, Giniatullin R, Klein RC, Fayuk D, Yakel JL. Functional mapping and Ca2+ regulation of nicotinic acetylcholine receptor channels in rat hippocampal CA1 neurons. J Neurosci. 2003; 23:9024–9031. [PubMed: 14534236]

Klausberger T, Magill PJ, Marton LF, Roberts JD, Cobden PM, Buzsaki G, Somogyi P. Brain-state- and cell-type-specific firing of hippocampal interneurons in vivo. Nature. 2003; 421:844–848. [PubMed: 12594513]

Kullmann DM, Lamsa KP. Long-term synaptic plasticity in hippocampal interneurons. Nat Rev Neurosci. 2007; 8:687–699. [PubMed: 17704811]

Kullmann DM, Lamsa K. Roles of distinct glutamate receptors in induction of anti-Hebbian long-term potentiation. J Physiol (Lond). 2008; 586:1481–1486. [PubMed: 18187472]

Lamsa KP, Heeroma JH, Somogyi P, Rusakov DA, Kullmann DM. Anti-Hebbian long-term potentiation in the hippocampal feedback inhibitory circuit. Science. 2007; 315:1262–1266. [PubMed: 17332410]

Lapointe V, Morin F, Ratté S, Croce A, Conquet F, Lacaille JC. Synapse-specific mGluR1-dependent long-term potentiation in interneurones regulates mouse hippocampal inhibition. J Physiol (Lond). 2004; 555:125–135. [PubMed: 14673190]

Lerma J, Paternain AV, Rodríguez-Moreno A, López-García JC. Molecular physiology of kainate receptors. Physiol Rev. 2001; 81:971–998. [PubMed: 11427689]

Levin ED. Nicotinic receptor subtypes and cognitive function. J Neurobiol. 2002; 53:633–640. [PubMed: 12436426]

Levin ED, Simon BB. Nicotinic acetylcholine involvement in cognitive function in animals. Psychopharmacology. 1998; 138:217–230. [PubMed: 9725745]

Lujan R, Nusser Z, Roberts JD, Shigemoto R, Somogyi P. Perisynaptic location of metabotropic glutamate receptors mGluR1 and mGluR5 on dendrites and dendritic spines in the rat hippocampus. Eur J Neurosci. 1996; 8:1488–1500. [PubMed: 8758956]

Maccaferri G, Roberts JDB, Szucs P, Cottingham CA, Somogyi P. Cell surface domain specific postsynaptic currents evoked by identified GABAergic neurons in rat hippocampus in vitro. J Physiol (Lond). 2000; 524:91–116. [PubMed: 10747186]

Maccaferri G. Stratum oriens horizontal interneurone diversity and hippocampal network dynamics. J Physiol (Lond). 2005; 562:73–80. [PubMed: 15498801]

Mann EO, Greenfield SA. Novel modulatory mechanisms revealed by the sustained application of nicotine in the guinea-pig hippocampus in vitro. J Physiol (Lond). 2003; 551:539–550. [PubMed: 12815181]

Marti Barros D, Ramirez MR, Dos Reis EA, Izquierdo I. Participation of hippocampal nicotinic receptors in acquisition, consolidation and retrieval of memory for one trial inhibitory avoidance in rats. Neuroscience. 2004; 126:651–656. [PubMed: 15183514]

Masu M, Tanabe Y, Tsuchida K, Shigemoto R, Nakanishi S. Sequence and expression of a metabotropic glutamate receptor. Nature. 1991; 349:760–765. [PubMed: 1847995]

Matsuyama S, Matsumoto A, Enomoto T, Nishizaki T. Activation of nicotinic acetylcholine receptors induces long-term potentiation *in vivo* in the intact mouse dentate gyrus. Eur J Neurosci. 2000; 12:3741–3747. [PubMed: 11029644]

McQuiston AR, Madison DV. Nicotinic receptor activation excites distinct subtypes of interneurons in the rat hippocampus. J Neurosci. 1999; 19:2887–2896. [PubMed: 10191306]

Nakauchi S, Brennan RJ, Boulter J, Sumikawa K. Nicotine gates long-term potentiation in the hippocampal CA1 region via the activation of alpha2* nicotinic ACh receptors. Eur J Neurosci. 2007a; 25:2666–2681. [PubMed: 17466021]

Nakauchi S, Yamazaki Y, Sumikawa K. Chronic nicotine exposure affects the normal operation of hippocampal circuits. NeuroReport. 2007b; 18:87–91. [PubMed: 17259867]

Oren I, Nissen W, Kullmann DM, Somogyi P, Lamsa KP. Role of ionotropic glutamate receptors in long-term potentiation in rat hippocampal CA1 oriens-lacunosum moleculare interneurons. J Neurosci. 2009; 29:939–950. [PubMed: 19176803]

Parra P, Gulyas AI, Miles R. How many subtypes of inhibitory cells in the hippocampus? Neuron. 1998; 20:983–993. [PubMed: 9620702]

Perez Y, Morin F, Lacaille JC. A hebbian form of long-term potentiation dependent on mGluR1a in hippocampal inhibitory interneurons. Proc Natl Acad Sci USA. 2001; 98:9401–9406. [PubMed: 11447296]

Pin JP, Duvoisin R. The metabotropic glutamate receptors: structure and functions. Neuropharmacology. 1995; 34:1–26. [PubMed: 7623957]

Role LW, Berg DK. Nicotinic receptors in the development and modulation of CNS synapses. Neuron. 1996; 16:1077–1085. [PubMed: 8663984]

Sawada S, Yamamoto C, Ohno-Shosaku T. Long-term potentiation and depression in the dentate gyrus, and effects of nicotine. Neurosci Res. 1994; 20:323–329. [PubMed: 7870386]

Seguela P, Wadiche J, Dineley-Miller K, Dani JA, Patrick JW. Molecular cloning, functional properties, and distribution of rat brain alpha 7: a nicotinic cation channel highly permeable to calcium. J Neurosci. 1993; 13:596–604. [PubMed: 7678857]

Somogyi P, Klausberger T. Defined types of cortical interneurone structure space and spike timing in the hippocampus. J Physiol (Lond). 2005; 562:9–26. [PubMed: 15539390]

Sudweeks SN, Yakel JL. Functional and molecular characterization of neuronal nicotinic ACh receptors in rat CA1 hippocampal neurons. J Physiol (Lond). 2000; 527:515–528. [PubMed: 10990538]

Topolnik L, Congar P, Lacaille JC. Differential regulation of metabotropic glutamate receptor- and AMPA receptor-mediated dendritic Ca^{2+} signals by presynaptic and postsynaptic activity in hippocampal interneurons. J Neurosci. 2005; 25:990–1001. [PubMed: 15673681]

Topolnik L, Azzi M, Morin F, Kougioumoutzakis A, Lacaille JC. mGluR1/5 subtype-specific calcium signalling and induction of long-term potentiation in rat hippocampal oriens/alveus interneurones. J Physiol (Lond). 2006; 575:115–131. [PubMed: 16740609]

Wada E, Wada K, Boulter J, Deneris E, Heinemann S, Patrick J, Swanson LW. Distribution of alpha 2, alpha 3, alpha 4, and beta 2 neuronal nicotinic receptor subunit mRNAs in the central nervous system: a hybridization histochemical study in the rat. J Comp Neurol. 1989; 284:314–335. [PubMed: 2754038]

Wanaverbecq N, Semyanov A, Pavlov I, Walker MC, Kullmann DM. Cholinergic axons modulate GABAergic signaling among hippocampal interneurons via postsynaptic alpha 7 nicotinic receptors. J Neurosci. 2007; 27:5683–5693. [PubMed: 17522313]

Welsby P, Rowan M, Anwyl R. Nicotinic receptor-mediated enhancement of long-term potentiation involves activation of metabotropic glutamate receptors and ryanodine-sensitive calcium stores in the dentate gyrus. Eur J Neurosci. 2006; 24:3109–3118. [PubMed: 17156372]

Woodhall G, Gee CE, Robitaille R, Lacaille JC. Membrane potential and intracellular Ca^{2+} oscillations activated by mGluRs in hippocampal stratum oriens/alveus interneurons. J Neurophysiol. 1999; 81:371–382. [PubMed: 9914296]

Yamazaki Y, Jia Y, Hamaue N, Sumikawa K. Nicotine-induced switch in the nicotinic cholinergic mechanisms of facilitation of long-term potentiation. Eur J Neurosci. 2005; 22:845–860. [PubMed: 16115208]

Yamazaki Y, Fujii S, Jia Y, Sumikawa K. Nicotine withdrawal suppresses nicotinic modulation of long-term potentiation induction in the hippocampal CA1 region. Eur J Neurosci. 2006b; 24:2903–2916. [PubMed: 17156213]

Zhang J, Berg DK. Reversible inhibition of GABAA receptors by alpha7-containing nicotinic receptors on the vertebrate postsynaptic neurons. J Physiol (Lond). 2007; 579:753–763. [PubMed: 17204496]

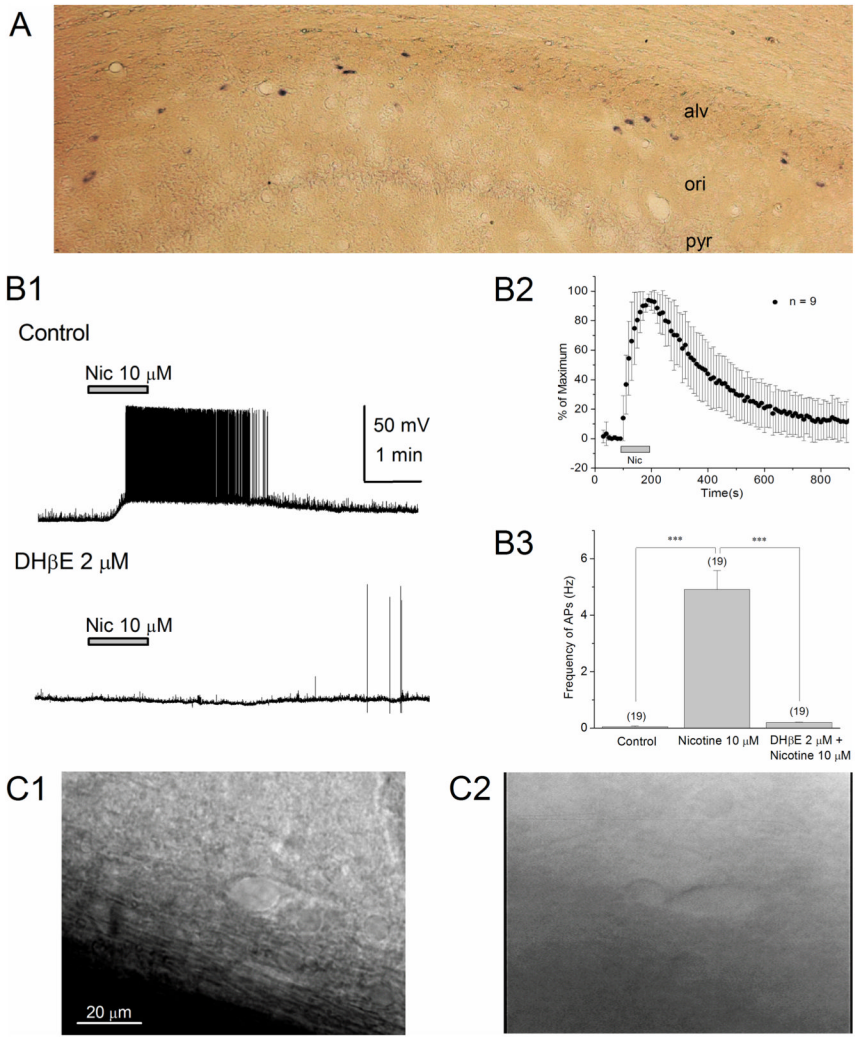

Figure 1. Horizontally oriented interneurons at the stratum oriens/alveus border are nicotine-sensitive

(A) Localization of α2 mRNA-containing interneurons in the hippocampal CA1 region by non-radioactive in situ hybridization. (B1) Bath application of nicotine (10 μM) in the presence of DNQX (20 μM) and AP5 (40 μM) increased the frequency of action potentials in current-clamped oriens/alveus interneurons, which was blocked by the non-α7 nAChR antagonist DHβE (2 μM). (B2) Summary plot of the effect of nicotine (10 μM) on the frequency of action potentials. The nicotine-induced change in the frequency of action potentials was normalized as a percentage change from the highest frequency of action potentials and was plotted against time. (B3) Summary plot of the effect of nicotine (10 μM) on the frequency of action potentials (mean ± SEM) in the absence and presence of DHβE (2 μM). Numbers in parentheses in this and the following figures indicate the numbers of experiments. (C1, C2) IR-DIC images of nicotine-sensitive oriens/alveus interneurons. These interneurons were covered by perineuronal glial cells (C1, the plane of focus was at the neuron under glial cells) or associated with perineuronal glial cells (C2). ***$P < 0.001$.

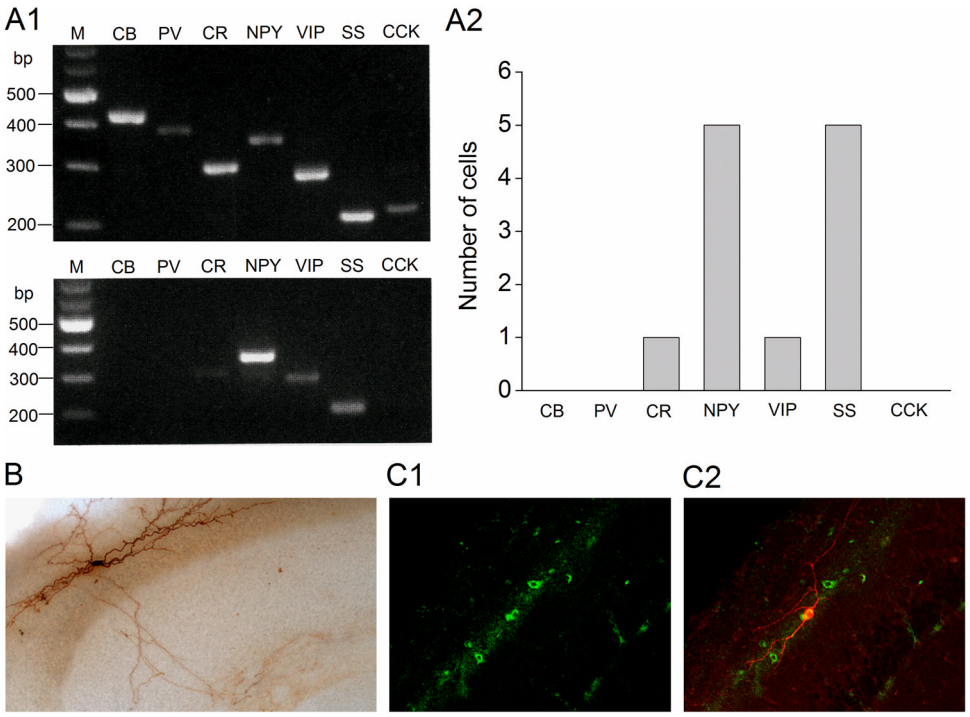

Figure 2. A subtype of nicotine-sensitive oriens/alveus interneurons and its molecular markers

(A1, A2) Nicotine-sensitive interneurons contain somatostatin and neuropeptide Y mRNAs. (A1, top) RT-multiplex PCR amplification of different marker sequences. Hippocampal RNA (500 pg) was subjected to a RT-multiplex PCR protocol to detect the expression of calbindin D28k (CB), parvalbumin (PV), calretinin (CR), neuropeptide Y (NPY), vasoactive intestinal polypeptide (VIP), somatostatin (SS), and cholecystokinin (CCK). (A1, bottom) RT-multiplex PCR applied on a single nicotine-sensitive interneuron after electrophysiological recording to detect molecular markers. An example of single-cell RT-multiplex PCR, showing the presence of CR, NPY, VIP, and SS in a recorded cell. RT-PCR products were separated by agarose gel electrophoresis and visualized with ethidium bromide. The amplified fragments had the sizes (in bp) predicted by the mRNA sequences: 432 (CB), 388 (PV), 309 (CR), 359 (NPY), 287 (VIP), 209 (SS), 216 (CCK). A 100 bp DNA ladder was used as a molecular weight marker. (A2) Summary data of single-cell RT-multiplex PCR. (B) One biocytin-labeled nicotine-sensitive interneuron with characteristics resembling oriens-lacunosum moleculare cells. (C1, C2) Double-labeling of a nicotine-sensitive interneuron with biocytine and immunohistochemistry for somatostatin. Immunohistochemical localization of somatostatin-containing interneurons (C1) and co-localization of somatostatin (green) and biocytin (red) in a nicotine-sensitive interneuron (C2).

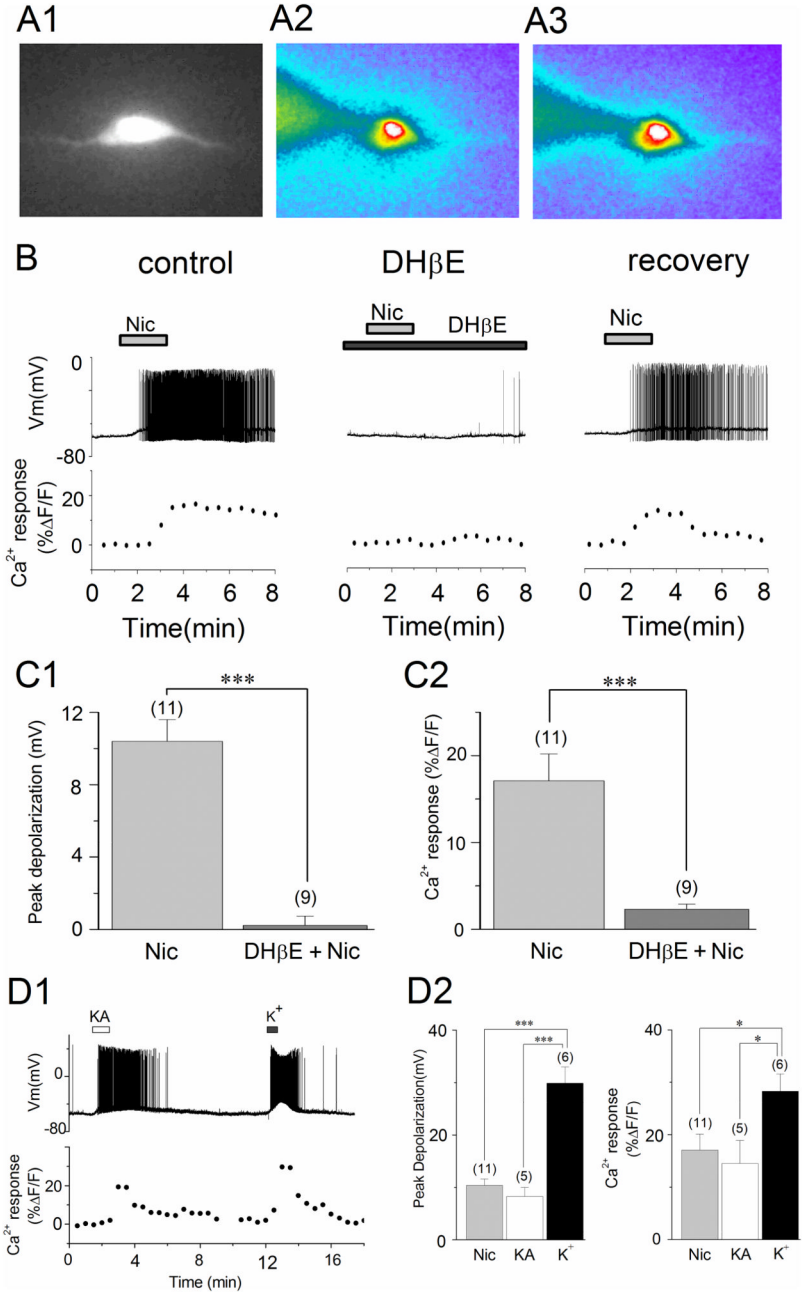

Figure 3. Nicotine increases intracellular Ca^{2+} concentrations in oriens/alveus interneurons via activation of non-α7 nAChRs

(A1–A3) Visualization of the fluorescent signal in oriens/alveus interneurons loaded with the Ca^{2+} indicator dye calcium green-1 through the recording pipette. (A1) A visualized oriens/alveus interneuron after dye loading. (A2, A3) Pseudo-color fluorescence imaging of a current-clamped oriens/alveus interneuron in the absence (A2) and presence (A3) of 10 μM nicotine. **Note that application of nicotine produced detectable increases in fluorescent intensity at the soma.** (B) Simultaneous recordings of electrical activity (Vm) and changes in Ca^{2+} fluorescence signal in a current-clamped oriens/alveus interneuron. Nicotine (10 μM; Nic)-induced changes in Vm and Ca^{2+} fluorescence signal were recorded in the absence (left) and presence of DHβE (2 μM; center) and 10 min after washout of

DHβE (right). Recordings were carried out in the presence of DNQX (20 μM) and AP5 (40 μM). (C1) Summary graph showing the magnitude of depolarization observed in the presence of nicotine (10 μM) and nicotine (10 μM) + DHβE (2 μM). (C2) Summary graph showing Ca^{2+} fluorescence signal observed in the presence of nicotine (10 μM) and nicotine (10 μM) + DHβE (2 μM). (D1) Kainate (1 μM; KA)- and K^+ (30 mM)-induced changes in Vm and Ca^{2+} fluorescence signal were simultaneously recorded. (D2) Summary graphs showing the magnitude of depolarization (left) and Ca^{2+} fluorescence signal (right) elicited by bath application of nicotine (10 μM), kainate (1 μM), and K^+ (30 mM). *$P < 0.05$, ***$P < 0.001$.

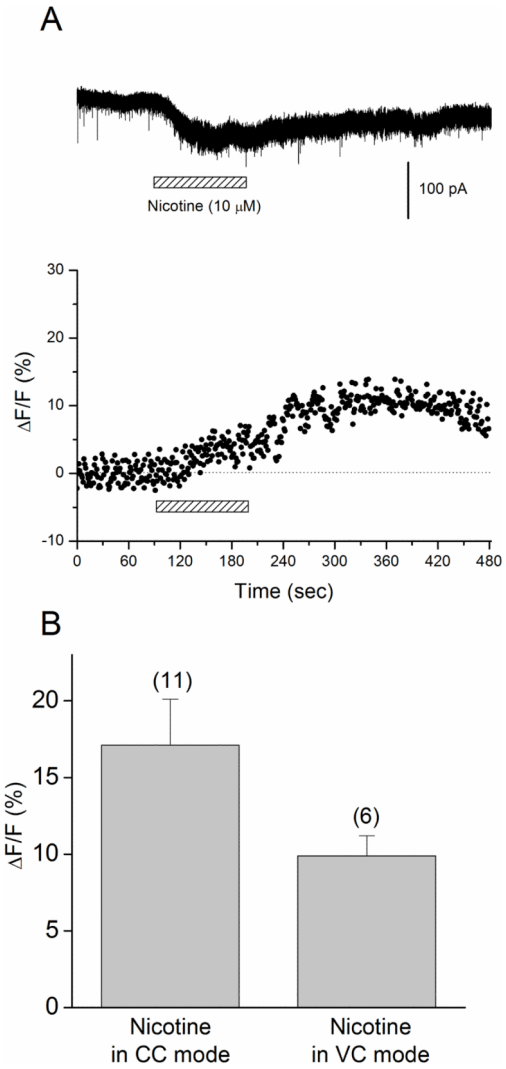

Figure 4. Nicotine elevates intracellular Ca^{2+} levels in oriens/alveus interneurons via Ca^{2+} entry through non-α7 nAChRs

(A) Simultaneous recordings of nicotine-induced currents (top) and changes in Ca^{2+} fluorescence signal (bottom) in a voltage-clamped oriens/alveus interneuron (at −70 mV). Recordings were carried out in the presence of DNQX (20 μM) and AP5 (40 μM). Nicotine (10 μM) was bath-applied as indicated by the horizontal bar. (B) Summary graph showing Ca^{2+} fluorescence signal (mean ± SEM) elicited in current-clamped (CC) and voltage-clamped (VC) oriens/alveus interneurons by bath application of nicotine (10 μM).

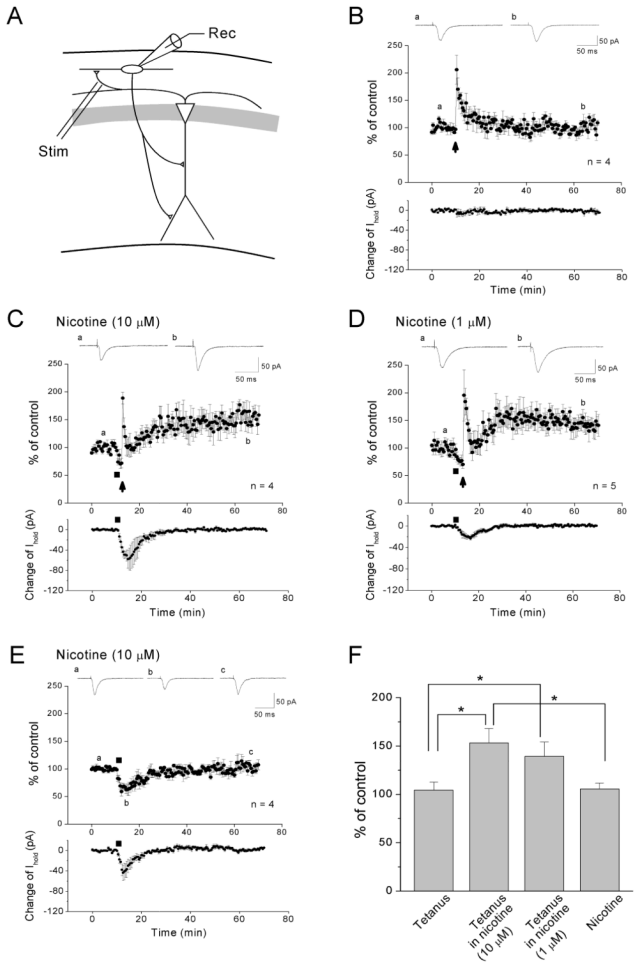

Figure 5. Nicotine promotes the induction of LTP at excitatory synapses onto oriens/alveus interneurons

(A) Scheme of recording setup showing the position of stimulating and recording electrodes. Oriens/alveus interneurons were voltage-clamped at −70 mV, and evoked EPSCs were recorded in the presence of AP5 (50 μM), bicuculline (10 μM), MLA (50 nM), and atropine (1 μM). (B–E) Changes in the amplitude of EPSCs were plotted as the percent change of initial baseline responses against time. Each trace above the graph in (B–E) was recorded at the time indicated. (B) A tetanus (100 pulses at 100Hz) alone failed to induce LTP. (C) A tetanus applied in the presence of nicotine (10 μM) induced LTP. (D) A tetanus applied in the presence of nicotine (1 μM) induced LTP. (E) Application of nicotine (10 μM) alone had no long-lasting effect on the amplitude of EPSCs. (C-E) Bath application of nicotine caused decreases in the amplitude of EPSCs (top) and increases in holding current (bottom). Administration of nicotine is indicated by the bar and delivery of tetanic stimulation is indicated by the arrow. (F) Histograms show the percent change (mean ± SEM) in the amplitude of EPSCs measured 50–60 min after delivery of tetanic stimulation in the absence and presence of nicotine, or after application of nicotine alone. *$P < 0.05$.

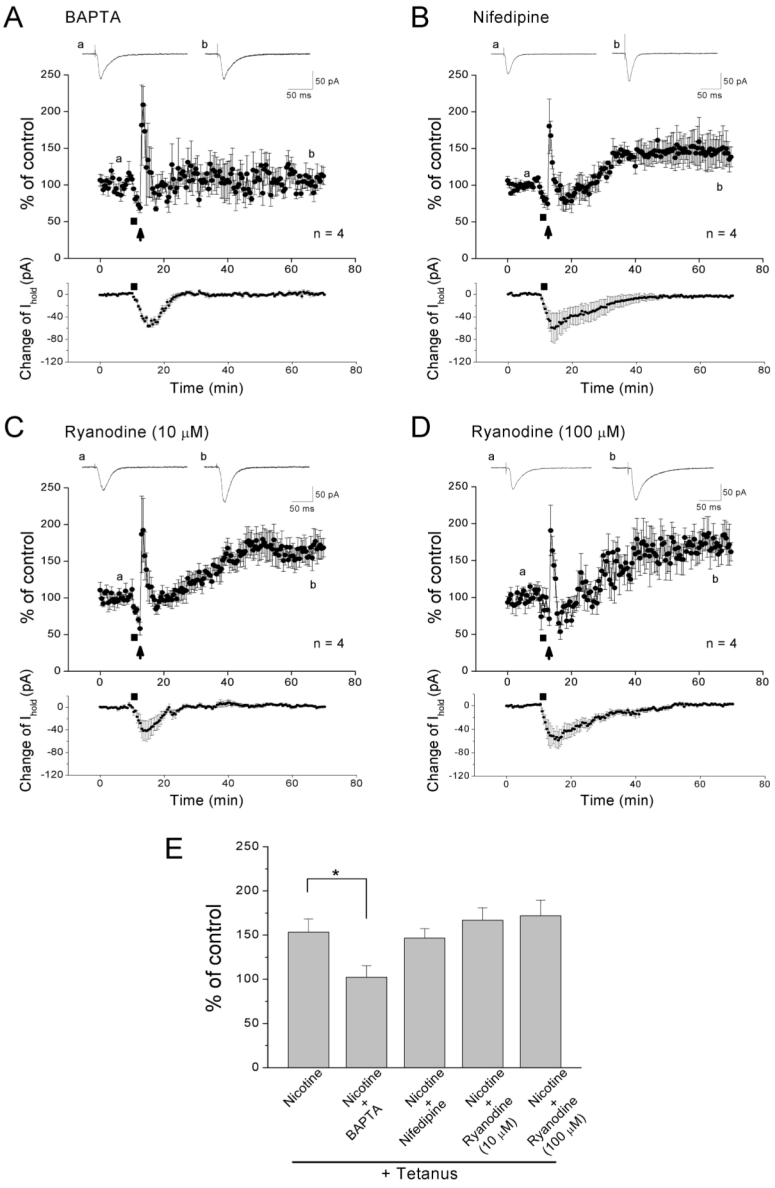

Figure 6. Ca^{2+} entry through non-α7 nAChRs facilitates LTP induction

Oriens/alveus interneurons were voltage-clamped at −70 mV, and evoked EPSCs were recorded in the presence of AP5 (50 μM), bicuculline (10 μM), MLA (50 nM), and atropine (1 μM). (A–D) Changes in the amplitude of EPSCs were plotted as the percent change of initial baseline responses against time. Each trace above the graph in (A–D) was recorded at the time indicated. (A) Nicotine-induced facilitation of LTP induction was blocked by intracellular perfusion of the calcium chelator BAPTA through the recording pipette (10 mM). (B) Nicotine still promoted LTP induction in the presence of nifedipine (30 μM). (C, D) Nicotine still facilitated LTP induction in the presence of 10 μM (C) and 100 μM (D) of ryanodine. (A–D) Bath application of nicotine caused decreases in the amplitude of EPSCs (top) and increases in holding current (bottom). Nifedipine (30 μM) or ryanodine (10 μM) was present throughout the entire recording period in (B) or (C), respectively. In the case of 100 μM ryanodine (D), the drug was present until 5 min after tetanus. Administration of nicotine is indicated by the bar and delivery of tetanic stimulation (100 pulses at 100Hz) is

indicated by the arrow. (E) Histograms show the percent change (mean ± SEM) in the amplitude of EPSCs measured 50–60 min after delivery of tetanic stimulation, to compare the effects of different drugs on nicotine-induced facilitation of LTP induction. *$P < 0.05$.